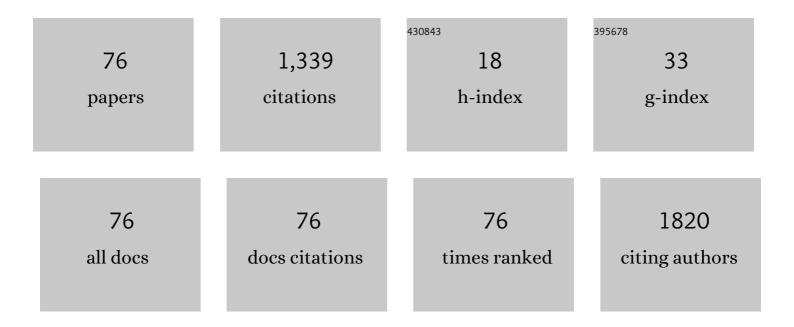
Hongtao Cui

List of Publications by Year in descending order

Source: https://exaly.com/author-pdf/311373/publications.pdf Version: 2024-02-01



#	Article	IF	CITATIONS
1	Structure switch between α-Fe2O3, γ-Fe2O3 and Fe3O4 during the large scale and low temperature sol–gel synthesis of nearly monodispersed iron oxide nanoparticles. Advanced Powder Technology, 2013, 24, 93-97.	4.1	201
2	MOF derived in-situ carbon-encapsulated Fe3O4@C to mediate polysulfides redox for ultrastable Lithium-sulfur batteries. Chemical Engineering Journal, 2020, 381, 122652.	12.7	106
3	Strategies of Large Scale Synthesis of Monodisperse Nanoparticles. Recent Patents on Nanotechnology, 2009, 3, 32-41.	1.3	68
4	Synergistic regulation of polysulfides immobilization and conversion by MOF-derived CoP-HNC nanocages for high-performance lithium-sulfur batteries. Nano Energy, 2021, 85, 106011.	16.0	68
5	Frogspawn inspired hollow Fe ₃ C@N–C as an efficient sulfur host for high-rate lithium–sulfur batteries. Nanoscale, 2019, 11, 21532-21541.	5.6	58
6	Large scale selective synthesis of α-Co(OH)2 and β-Co(OH)2 nanosheets through a fluoride ions mediated phase transformation process. Journal of Alloys and Compounds, 2013, 562, 33-37.	5.5	41
7	Structure control synthesis of iron oxide polymorph nanoparticles through an epoxide precipitation route. Journal of Experimental Nanoscience, 2013, 8, 869-875.	2.4	40
8	Large scale synthesis of highly crystallized SnO ₂ quantum dots at room temperature and their high electrochemical performance. Nanotechnology, 2013, 24, 345602.	2.6	35
9	Self-templating synthesis of prismatic-like N-doped carbon tubes embedded with Fe3O4 as a high-efficiency polysulfide-anchoring-conversion mediator for high performance lithium-sulfur batteries. Chemical Engineering Journal, 2021, 410, 128153.	12.7	33
10	Large-scale synthesis of Fe9S10/Fe3O4@C heterostructure as integrated trapping-catalyzing interlayer for highly efficient lithium-sulfur batteries. Chemical Engineering Journal, 2021, 422, 130049.	12.7	31
11	Ultra-high specific capacitance of β-Ni(OH)2 monolayer nanosheets synthesized by an exfoliation-free sol–gel route. Journal of Nanoparticle Research, 2014, 16, 1.	1.9	28
12	Facile and ultra large scale synthesis of nearly monodispersed CoFe2O4 nanoparticles by a low temperature sol–gel route. Journal of Sol-Gel Science and Technology, 2010, 55, 36-40.	2.4	26
13	Low temperature and size controlled synthesis of monodispersed γ-Fe2O3 nanoparticles by an epoxide assisted sol–gel route. Journal of Sol-Gel Science and Technology, 2008, 47, 81-84.	2.4	24
14	A chemical strategy to control the shape of oxide nanoparticles. Journal of Nanoparticle Research, 2009, 11, 1331-1338.	1.9	22
15	One-pot solvothermal synthesis of size-controlled NiO nanoparticles. Advanced Powder Technology, 2019, 30, 861-868.	4.1	22
16	One-pot synthesis of powder-form β-Ni(OH)2 monolayer nanosheets with high electrochemical performance. Journal of Nanoparticle Research, 2013, 15, 1.	1.9	21
17	Large-scale synthesis of paratacamite nanoparticles with controlled size and morphology. Micro and Nano Letters, 2011, 6, 823.	1.3	20
18	High rate performance and stabilized cycle life of Co2+-doped nickel sulfide nanosheets synthesized by a scalable method of solid-state reaction. Chemical Engineering Journal, 2019, 366, 33-40.	12.7	19

Ηονστάο Cui

#	Article	IF	CITATIONS
19	Synthesis of high electrochemical performance Ni(OH)2 nanosheets through a solvent-free reaction for application in supercapacitor. Advanced Powder Technology, 2015, 26, 434-438.	4.1	18
20	Ultra-large scale synthesis of Co–Ni layered double hydroxides monolayer nanosheets by a solvent-free bottom-up strategy. Journal of Alloys and Compounds, 2016, 662, 315-319.	5.5	18
21	Synthesis of Î'-MnO2 with nanoflower-like architecture by a microwave-assisted hydrothermal method. Journal of Sol-Gel Science and Technology, 2017, 82, 85-91.	2.4	17
22	Synthesis of nanostructured CoOOH film with high electrochemical performance for application in supercapacitor. Journal of Nanoparticle Research, 2014, 16, 1.	1.9	16
23	Facile synthesis of nickel–cobalt double hydroxide nanosheets with high rate capability for application in supercapacitor. Journal of Nanoparticle Research, 2015, 17, 1.	1.9	16
24	Hierarchical nanostructure-tuned super-high electrochemical stability of nickel cobalt sulfide. Journal of Materials Chemistry A, 2018, 6, 19788-19797.	10.3	16
25	Co2(OH)3Cl nanoparticles as new-type electrode material with high electrochemical performance for application in supercapacitor. Advanced Powder Technology, 2017, 28, 2642-2647.	4.1	15
26	Zn-Ion Batteries: Boosting the Rate Capability and Low-temperature Performance by Combining Structure and Morphology Engineering. ACS Applied Materials & Interfaces, 2021, 13, 34468-34476.	8.0	15
27	A bottom-up strategy for exfoliation-free synthesis of soluble α-Ni(OH) ₂ monolayer nanosheets on a large scale. RSC Advances, 2016, 6, 85367-85373.	3.6	14
28	Surfactant-free synthesis of water-soluble anatase nanoparticles and their application in preparation of high optic performance monoliths. Journal of Colloid and Interface Science, 2013, 398, 7-12.	9.4	13
29	High electrochemical performance of nanostructured CoOOH grown on nickel foam by hydrothermal deposition for application in supercapacitor. Journal of Sol-Gel Science and Technology, 2016, 79, 83-88.	2.4	13
30	Controlled microstructure in two dimensional Ni-Co LDH nanosheets-crosslinked network for high performance supercapacitors. Advanced Powder Technology, 2019, 30, 1239-1246.	4.1	13
31	Trapping and catalytic conversion of polysulfides by kirkendall effect built hollow NiCo2S4 nano-prisms for advanced sulfur cathodes in Li–S battery. Journal of Materials Science, 2021, 56, 4328-4340.	3.7	13
32	Ambient temperature sol–gel synthesis of CeO2–SiO2 and TiO2–CeO2–SiO2 films with high efficiency of UV absorption and without destructive oxidation on heat sensitive organic substrate. Journal of Sol-Gel Science and Technology, 2009, 50, 261-266.	2.4	12
33	Synthesis of nanofiber-composed dandelion-like CoNiAl triple hydroxide as an electrode material for high-performance supercapacitor. Journal of Nanoparticle Research, 2014, 16, 1.	1.9	12
34	Ultra-high rate capability of the synergistically built dual nanostructure of NiCo ₂ S ₄ /nickel foam as an electrode in supercapacitors. Nanoscale, 2020, 12, 22330-22339.	5.6	12
35	Shell-strengthened hollow architecture of NiCo2S4 carved through an in-situ reaction Ostwald Ripening mechanism with significantly enhanced electrochemical performance. Journal of Alloys and Compounds, 2021, 889, 161632.	5.5	12
36	New insight on nanostructure assembling of high-performance electrode materials: synthesis of surface-modified hexagonal β-Ni(OH)2 nanosheets as an example. Ionics, 2016, 22, 573-579.	2.4	11

Ηονστάο Cui

#	Article	IF	CITATIONS
37	Synthesis of periodically stacked 2D composite of α-Ni(OH)2 monolayer and reduced graphene oxide as electrode material for high performance supercapacitor. Advanced Powder Technology, 2018, 29, 631-638.	4.1	10
38	Studies on waterline corrosion processes and corrosion productÂcharacteristics of carbon steel in 3.5 wt% NaCl solution. Materials and Corrosion - Werkstoffe Und Korrosion, 2021, 72, 732-742.	1.5	10
39	Synthesis on an ultra large scale of nearly monodispersed γ-Fe2O3 nanoparticles with La(III) doping through a sol–gel route assisted by propylene oxide. Journal of Sol-Gel Science and Technology, 2010, 54, 37-41.	2.4	9
40	Aqueous foams stabilized solely by CoOOH nanoparticles and the resulting construction of hierarchically hollow structure. Journal of Nanoparticle Research, 2013, 15, 1.	1.9	9
41	Ultra-large scale synthesis of high electrochemical performance SnO2 quantum dots within 5min at room temperature following a growth self-termination mechanism. Journal of Alloys and Compounds, 2015, 645, 11-16.	5.5	9
42	Surfactant-free large scale synthesis of Co3O4 quantum dots at room temperature. Advanced Powder Technology, 2016, 27, 2019-2024.	4.1	9
43	Building an interpenetrating network of Ni(OH)2/reduced graphene oxide composite by a sol–gel method. Journal of Materials Science, 2018, 53, 15118-15129.	3.7	9
44	Low temperature transformation from γ-Fe2O3 to Ti doped α-Fe2O3 nanoparticles through an epoxide assisted sol–gel route. Journal of Sol-Gel Science and Technology, 2009, 51, 119-123.	2.4	8
45	Highly transparent silica monoliths embedded with high concentration oxide nanoparticles. Journal of Sol-Gel Science and Technology, 2013, 66, 512-517.	2.4	8
46	Promotion of electrochemical performance by tailoring the surface of β-Ni(OH)2 nanosheets. Journal of Sol-Gel Science and Technology, 2016, 78, 120-125.	2.4	8
47	High shear-granulated hierarchically porous spheres nanostructure-designed for high-performance supercapacitors. Advanced Powder Technology, 2019, 30, 2440-2449.	4.1	8
48	The key role of microscopic structure and graphene sheet-high homogenization in the high rate capability and cycling stability of Ni–Co LDH. Nanoscale, 2020, 12, 23799-23808.	5.6	8
49	Highly transparent UV absorption TiO2-SiO2-Fe2O3 films without oxidation catalytic activity prepared by a room temperature sol–gel route. Journal of Sol-Gel Science and Technology, 2011, 58, 476-480.	2.4	7
50	Exfoliation-free Nanosheet Synthesis of Transition-metal Hydroxynitrate and Its Transformation to Oxide Particulate Nanosheet. Chemistry Letters, 2007, 36, 144-145.	1.3	6
51	Template-free sol–gel synthesis of microporous NiO–SiO2 composite with high surface area and narrow pore size distribution. Journal of Sol-Gel Science and Technology, 2008, 47, 360-364.	2.4	6
52	Preparation of α-Co(OH)2 monolayer nanosheets by an intercalation agent-free exfoliation process. Journal of Sol-Gel Science and Technology, 2016, 78, 293-298.	2.4	6
53	Synthesis of CeO2 nanocrystals with controlled size and shape and their influence on electrochemical performance. Journal of Sol-Gel Science and Technology, 2017, 83, 308-314.	2.4	6
54	Micro-nano architecture with carbonaceous shell enables ultra-long cycling life of battery-type electrode materials in supercapacitors. Journal of Alloys and Compounds, 2022, 905, 164246.	5.5	6

Ηονςταο Cui

#	Article	IF	CITATIONS
55	Sol–gel preparation of highly transparent α-Fe2O3 film for the application in red color filter. Journal of Sol-Gel Science and Technology, 2011, 57, 20-23.	2.4	5
56	High water solubility and sol–gel transition behavior of titania nanoparticles obtained by an in situ functionalization sol–gel process. Journal of Sol-Gel Science and Technology, 2014, 70, 355-360.	2.4	5
57	Hierarchically structured nanofelt-like β-NiOOH grown on nickel foam as electrode for high performance pseudocapacitor. Journal of Nanoparticle Research, 2015, 17, 1.	1.9	5
58	Construction of cobalt substituted α-Ni(OH)2 hierarchical nanostructure from nanofibers on nickel foam and its electrochemical performance. Solid State Ionics, 2015, 281, 38-42.	2.7	5
59	Morphology and phase control of iron oxide polymorph nanoparticles. Materials Research Express, 2017, 4, 045006.	1.6	5
60	In situ template synthesis of SnO nanoparticles on nickel foam with high electrochemical performance. Journal of Sol-Gel Science and Technology, 2018, 86, 423-430.	2.4	5
61	Surface topography control of NiS/Ni3S4 nanosheets for the promotion of electrochemical performance. Journal of Sol-Gel Science and Technology, 2018, 87, 546-553.	2.4	5
62	In situ synthesis of two-dimensional Co2+-doped β-Ni(OH)2 using nickel complex as template for application in supercapacitors. Journal of Sol-Gel Science and Technology, 2019, 89, 492-499.	2.4	5
63	A branched nanosheet-interlaced structure of high performance Ni(OH)2 derived from the isostructural Ni3(NO3)2(OH)4 to clarify the role of structure self-supporting in cycling stability. Sustainable Energy and Fuels, 2020, 4, 1780-1788.	4.9	5
64	Branched nanosheets-interlaced structure of Co2+/Co3+-doped Ni(OH)2 originating from Ni3(NO3)2(OH)4 template with significantly boosted electrochemical performance. Journal of Materials Science, 2021, 56, 3011-3023.	3.7	5
65	A general ultra large scale strategy for low temperature sol–gel synthesis of nearly monodispersed metal ions doped l³-Fe2O3 nanoparticles. Journal of Sol-Gel Science and Technology, 2011, 58, 232-237.	2.4	4
66	Redispersity/Solubility of Nanopowder in Solvents. Recent Patents on Nanotechnology, 2014, 8, 18-30.	1.3	4
67	Oxidation effect of ammonium persulfate on the supercapacitive properties of βâ€Ni(OH) ₂ nanosheets. Physica Status Solidi (A) Applications and Materials Science, 2016, 213, 215-220.	1.8	4
68	Electrically conductive TiO2/indium tin oxide coated glass substrates with high visible light transparency prepared by an electrodeposition method. Thin Solid Films, 2019, 691, 137612.	1.8	4
69	Nanosheets self-supported structure in the orderly porous spheres of Co/Mn ions co-substituted α-Ni(OH)2 for high-performance supercapacitors. Journal of Sol-Gel Science and Technology, 2021, 97, 422-430.	2.4	3
70	Tailoring the size and electrochemical performance of Mn3O4 nanoparticles by controlling the precipitation process. Journal of Sol-Gel Science and Technology, 2016, 80, 326-332.	2.4	2
71	Graphitic SiC : A potential anode material for Naâ€ion battery with extremely high storage capacity. International Journal of Quantum Chemistry, 2021, 121, e26608.	2.0	2
72	Building homogeneous nanostructure in Ni(OH) ₂ /MWCNTs composite by electrostatic attraction. Micro and Nano Letters, 2019, 14, 1151-1156.	1.3	2

Ηονστάο Cui

#	Article	IF	CITATIONS
73	Assembly of Ni(OH)2-based electrodes without material synthesis step for application in supercapacitors. Journal of Sol-Gel Science and Technology, 2018, 85, 349-355.	2.4	1
74	Nanoengineered Skeletonâ€surface of Nickel Foam with Additional Dual Functions of Rateâ€capability Promotion and Cyclingâ€life Stabilization for Nickel Sulfide Electrodes. ChemNanoMat, 2020, 6, 1365-1372.	2.8	1
75	Basic cadmium salts as phaseâ€directing agent for the phase and morphology control of metal hydroxychlorides. Micro and Nano Letters, 2017, 12, 285-288.	1.3	1
76	Emulsionâ€Tailored Pore Properties and Electrochemical Performance of Ni(OH) 2 Spheres Using High Shear as Driving Force. Physica Status Solidi (A) Applications and Materials Science, 2020, 217, 2000135.	1.8	0